

Sorption of Poly- and Perfluoroalkyl Substances (PFASs) Relevant to Aqueous Film-Forming Foam (AFFF)-Impacted Groundwater by Biochars and Activated Carbon

Xin Xiao,^{†,‡,§} Bridget A. Ulrich,[‡] Baoliang Chen,^{†,§} and Christopher P. Higgins^{*,‡,§}

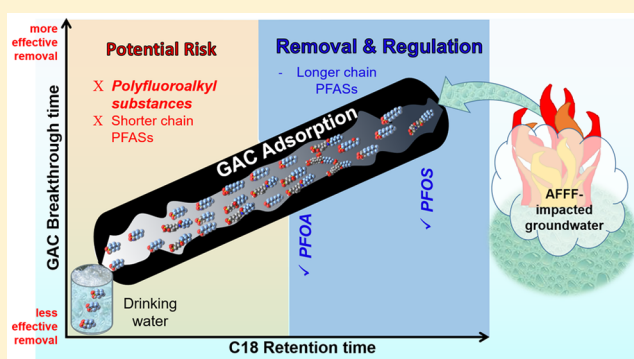
[†]Department of Environmental Science, Zhejiang University, Hangzhou 310058, China

[‡]Department of Civil and Environmental Engineering, Colorado School of Mines, Golden, Colorado 80401, United States

[§]Zhejiang Provincial Key Laboratory of Organic Pollution Process and Control, Hangzhou 310058, China

Supporting Information

ABSTRACT: Despite growing concerns about human exposure to perfluorooctanoate (PFOA) and perfluorooctanesulfonate (PFOS), other poly- and perfluoroalkyl substances (PFASs) derived from aqueous film-forming foams (AFFFs) have garnered little attention. While these other PFASs may also be present in AFFF-impacted drinking water, their removal by conventional drinking-water treatment is poorly understood. This study compared the removal of 30 PFASs, including 13 recently discovered PFASs, from an AFFF-impacted drinking water using carbonaceous sorbents (i.e., granular activated carbon, GAC). The approach combined laboratory batch experiments and modeling: batch sorption data were used to determine partition coefficients (K_d) and calibrate a transport model based on intraparticle diffusion-limited sorption kinetics, which was used to make forward predictions of PFAS breakthrough during GAC adsorption. While strong retention was predicted for PFOS and PFOA, nearly all of the recently discovered polyfluorinated chemicals and PFOS-like PFASs detected in the AFFF-impacted drinking water were predicted to break through GAC systems before both PFOS and PFOA. These model breakthrough results were used to evaluate a simplified approach to predicting PFAS removal by GAC using compound-specific retention times on a C18 column (RT_{C18}). Overall, this study reveals that GAC systems for the treatment of AFFF-impacted sources of water for PFOA and PFOS likely achieve poor removal, when operated only for the treatment of PFOS and PFOA, of many unmonitored PFASs of unknown toxicity.



INTRODUCTION

Aqueous film-forming foams (AFFFs) were developed to quickly extinguish hydrocarbon fuel fires at military bases, airports, and oil refineries, and have been used for training and emergency response situations at such locations.¹ While the presence of perfluorinated surfactants in AFFF has been known for some time,^{1–3} the relative importance of polyfluorinated compounds has only recently garnered significant attention.^{4–7} When released to the environment, these poly- and perfluoroalkyl substances (PFASs) can lead to soil and groundwater contamination and subsequent public health concerns due to their persistent and bioaccumulative nature.^{1,8–11} Human exposure to PFASs due to contaminated drinking water has recently become an area of particular concern: on May 19th of 2016, the U.S. Environmental Protection Agency (EPA) issued drinking water health advisories levels (HALs) for two PFASs, perfluorooctanoate (PFOA) and perfluorooctanesulfonate (PFOS), of 70 ng/L (individually or combined).¹² These HALs were issued out of concern that exposure to PFOS or PFOA may result in

development effects, liver effects, impaired immune system function, or cancer.¹³ Hu et al. estimated, using the EPA's Unregulated Contaminant Monitoring Rule (UCMR) data,¹⁴ that 6 million people in the United States may have been exposed to PFAS levels exceeding these HALs,⁴ with some evidence to suggest that AFFF releases are at least partly responsible for the widespread contamination of drinking water with PFASs. One study used these same EPA data to correlate potential for exposure through drinking water to blood serum levels,¹⁵ while others have suggested these HALs are not conservative enough.^{16,17} For example, Vermont has issued a Ground Water Standard for the sum of PFOA and PFOS of 20 ng/L.¹⁸

Despite the growing concerns about human exposure to PFOS and PFOA, there is a lack of information on exposure to

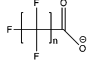
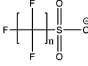
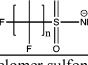
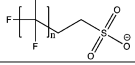
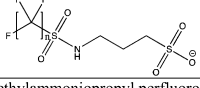
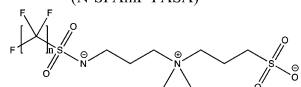
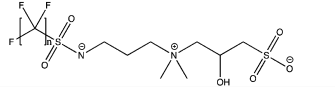
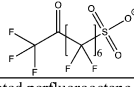
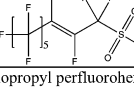
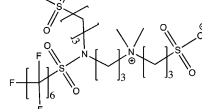
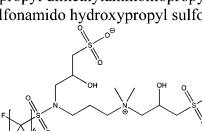
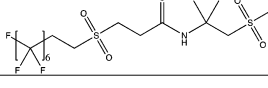
Received: February 22, 2017

Revised: May 9, 2017

Accepted: May 16, 2017

Published: June 6, 2017

Table 1. Poly- and Perfluoroalkyl Substances (PFASs) Included in This Study

Compound Class and Structure	Perfluoroalkyl Chain Length (n)	Compound	Formula	m/z	Analysis ^a
Perfluorocarboxylate (PFCA) 	3	PFBA	C ₄ F ₇ O ₂ ⁻	212.9787	MS/MS
	4	PFPeA	C ₅ F ₉ O ₂ ⁻	262.9755	MS/MS
	5	PFHxA	C ₆ F ₁₁ O ₂ ⁻	312.9723	MS/MS
	6	PFHpA	C ₇ F ₁₃ O ₂ ⁻	362.9691	MS/MS
	7	PFOA	C ₈ F ₁₅ O ₂ ⁻	412.9659	MS/MS
Perfluorosulfonate (PFSA) 	3	PFPrS	C ₃ F ₅ SO ₃ ⁻	248.9456	Q-ToF
	4	PFBS	C ₄ F ₇ SO ₃ ⁻	298.9424	MS/MS
	5	PFPeS	C ₅ F ₉ SO ₃ ⁻	348.9393	Q-ToF
	6	PFHxS	C ₆ F ₁₁ SO ₃ ⁻	398.9361	MS/MS
	7	PFHpS	C ₇ F ₁₃ SO ₃ ⁻	448.9329	MS/MS
Perfluoroalkyl sulfonamide (FASA) 	3	FPrSA	C ₃ HF ₇ NSO ₂ ⁻	247.9616	Q-ToF
	4	FBSA	C ₄ HF ₉ NSO ₂ ⁻	297.9584	Q-ToF
	5	FPeSA	C ₅ HF ₁₁ NSO ₂ ⁻	347.9552	Q-ToF
	6	FHxSA	C ₆ HF ₁₃ NSO ₂ ⁻	397.9520	Q-ToF
Fluorotelomer sulfonate (FtS) 	4	4:2 FtS	C ₆ H ₄ F ₆ SO ₃ ⁻	326.9737	Q-ToF
	6	6:2 FtS	C ₈ H ₄ F ₁₀ SO ₃ ⁻	426.9674	Q-ToF
N-sulfopropyl perfluoroalkanesulfonamide (N-SP-FASA) 	4	N-SP-FBSA	C ₇ H ₇ F ₉ NS ₂ O ₅ ⁻	419.9622	Q-ToF
	5	N-SP-FPeSA	C ₈ H ₇ F ₁₁ NS ₂ O ₅ ⁻	469.9590	Q-ToF
	6	N-SP-FHxSA	C ₉ H ₇ F ₁₃ NS ₂ O ₅ ⁻	519.9558	Q-ToF
N-sulfopropyl dimethylammonio propyl perfluoroalkane sulfonamide (N-SPAmP-FASA) 	4	N-SPAmP-FBSA	C ₁₂ H ₁₈ F ₉ N ₂ S ₂ O ₅ ⁻	505.0513	Q-ToF
	5	N-SPAmP-FPeSA	C ₁₃ H ₁₈ F ₁₁ N ₂ S ₂ O ₅ ⁻	555.0482	Q-ToF
	6	N-SPAmP-FHxSA	C ₁₄ H ₁₈ F ₁₃ N ₂ S ₂ O ₅ ⁻	605.0450	Q-ToF
N-sulfohydroxypropyl dimethylammonio propyl perfluoroalkane sulfonamide (N-SHOPAmP-FASA) 	4	N-SHOPAmP-FBSA	C ₁₂ H ₁₈ F ₉ N ₂ S ₂ O ₆ ⁻	521.0463	Q-ToF
	6	N-SHOPAmP-FHxSA	C ₁₄ H ₁₈ F ₁₃ N ₂ S ₂ O ₆ ⁻	621.0399	Q-ToF
Compound Name and Structure		Compound	Formula	m/z	Analysis^a
Keto-perfluorooctanesulfonate ^b 		7K-PFOS	C ₈ F ₁₅ SO ₄ ⁻	476.9278	Q-ToF
Unsaturated perfluorooctane sulfonate ^c 		U-PFOS	C ₈ F ₁₅ SO ₃ ⁻	460.9329	Q-ToF
N-sulfopropyl dimethylammonio propyl perfluorohexane sulfonamide propylsulfonate 		N-SPAmP-FHxSAPS	C ₁₇ H ₂₄ F ₁₃ N ₂ S ₃ O ₈ ⁻	727.0487	Q-ToF
N-sulfohydroxypropyl dimethylammonio propyl perfluorohexane sulfonamido hydroxypropyl sulfonate 		N-SHOPAmP-FHxSAHOPS	C ₁₇ H ₂₄ F ₁₃ N ₂ S ₃ O ₁₀ ⁻	759.0386	Q-ToF
6:2 fluorohexyl sulfonyl propanoamido-methylpropylsulfonate 		6:2 FHxSO ₂ PA-MePS	C ₁₅ H ₁₇ F ₁₃ NS ₂ O ₆ ⁻	618.0290	Q-ToF

^aMS/MS: LC-MS/MS; Q-ToF: LC-Q-ToF-MS. For those PFASs analyzed by LC-MS/MS, the MS/MS transitions are provided in McKenzie et al.³⁷ ^bThe position of the ketone bond appears to be variable. ^cThe position of the double bond appears to be variable.

and toxicity of other PFASs, particularly the polyfluorinated compounds, which often are composed of perfluoroalkyl tails and nonfluorinated head groups. It is expected that many of these polyfluorinated compounds can be transformed, either in the environment or in humans, to the more-problematic perfluorocarboxylates (PFCAs) and perfluorosulfonates (PFASs).^{19–22} The full extent of PFASs present in AFFF and AFFF-impacted groundwater has only recently received

significant attention,^{7,23–25} although there is increasing evidence to suggest that perfluoroalkyl sulfonamides (FASAs) and other polyfluoroalkyl substances (likely chemical precursors to either PFCAs or PFASs) are commonly present in AFFF-impacted groundwater.^{6,25,26} Further, though often present at high concentrations, PFOA and PFOS are not always the most abundant PFASs in AFFF-impacted groundwaters.²⁷ While the toxicity of PFASs other than PFOA and

PFOS remains largely unexplored, some polyfluorinated compounds have exhibited higher toxicity than PFCAs in aquatic organisms.²⁸ Moreover, PFOS-like chemicals have been recently detected in AFFF-exposed firefighters,²⁹ raising questions about the bioaccumulation of PFOS-like PFASs.

When a water supply becomes contaminated with PFASs, several technologies may be applied to remove the PFASs and reduce human exposure, including reverse osmosis, nano-filtration, strong anion-exchange resins, and sorptive removal via granular activated carbon (GAC).^{30–35} The latter is particularly attractive, as GAC has been widely used to treat contaminated drinking water for many decades.^{36,37} Some have evaluated the sorptive removal of PFOA and PFOS using various carbonaceous sorbents in artificially spiked deionized water³⁸ or surface water.³¹ We are not aware of any studies in which PFAS sorption has been evaluated in systems containing polyfluorinated compounds relevant to AFFF-impacted groundwater, though the sorptive removal of perfluoroalkyl ether carboxylic acids (PFECAs) by powdered AC in a contaminated surface water was recently evaluated.³⁹ The polyfluorinated compounds are of interest not only because of the limited data on their toxicity but also because their presence, in addition to the source water chemistry,^{40,41} may impact GAC efficacy for PFOA and PFOS removal.

The objective of this study was to evaluate the potential for carbonaceous sorbents to remove a suite of PFASs, including newly discovered PFASs, from an AFFF-impacted groundwater. Due to the limited quantities of contaminated water available for shipping to the laboratory (~10 L), this was achieved primarily through batch experiments and modeling. First, the sorptive removal of PFASs was compared for several types of carbonaceous sorbents (i.e., two biochars and GAC). Then, equilibrium and kinetic batch data were used to calibrate a transport model based on intraparticle diffusion-limited sorption kinetics to describe sorption of a broad suite of AFFF-derived PFASs to GAC. Forward simulations were then evaluated for a full-scale GAC adsorption system to assess the treatability of the other PFASs relative to the more commonly monitored PFCAs and PFASs. Finally, a simple approach for predicting the breakthrough behavior of AFFF-derived PFASs in GAC adsorption systems was evaluated by relating predicted breakthrough times to chromatography retention times. Our results bring to light the importance of considering a broader suite of PFASs (including polyfluorinated precursors and PFOS-like PFASs) during GAC treatment of AFFF-impacted drinking water.

MATERIALS AND METHODS

Sorbents and Groundwater. The initially screened sorbents were the commercially available GAC Calgon Filtersorb300 (F300, Calgon Carbon Co., Pittsburgh, PA), pine needle (PN)-derived biochars produced at a range of temperatures (150, 250, 350, 500, and 700 °C; Table S1), and MCG biochar (Mountain Crest Gardens, Gropro Inc., Etna, CA). The high surface area (SA) materials F300 (997 m²/g SA) and MCG biochar (351 m²/g SA) were selected due to their demonstrated effectiveness for removal of stormwater trace organic contaminants in a previous study.⁴² F300 (F300-original, 0.8–1.0 mm effective particle size) was crushed and sieved into different particle size fractions (<53, 53–124, 124–180, 180–500, and >500 μm). Details related to the particle size fractions of F300 as well as the preparation of PN biochars are provided in the Supporting Information, and additional

properties of F300, MCG biochar, and PN-derived biochars are reported in Table S1. In this work, F300 refers to the F300-original unless the particle size is included in the label (i.e., F300 < 53 μm).

The AFFF-impacted groundwater was collected from a groundwater well at an AFFF-impacted site near a former military facility in the United States and was stored at 4 °C until use. General water quality parameters measured for filtered (0.45 μm) subsamples included pH (7.5), dissolved organic carbon (DOC, 46.0 ± 0.9 mg/L), dissolved metals (Na⁺, Ca²⁺, Mg²⁺, etc.), and anions (F⁻, Cl⁻, NO₂⁻, Br⁻, NO₃⁻, PO₄³⁻, and SO₄²⁻), all of which were measured using standard procedures (Sievers Total Organic Carbon Analyzer; ion chromatography, IC; and inductively coupled plasma atomic emission spectroscopy, ICP-AES, respectively; Table S2).

PFAS Identification and Quantification. Analysis of PFASs (Table 1) in the unfiltered groundwater was conducted via both liquid chromatography tandem mass spectrometry (LC–MS/MS; ABSciex API 3200) and LC–quadrupole time-of-flight MS (LC–QToF-MS; ABSciex 5600+). Sample preparation methods, MS/MS transitions, and calibration standards employed were similar to those described by McKenzie et al.,⁴³ with stable-isotope surrogate standards used whenever possible. For sample preparation, 1.3 mL of sample was transferred to a microcentrifuge tube and centrifuged at 16 000 RCF for 15 min. A subsample (0.26 mL) was then transferred to 2 mL autosampler vials containing 0.039 mL of basic water (0.01% NH₄OH) and 0.13 mL of surrogate (in 70% methanol), resulting in a final volume of 1.3 mL (containing 20% (V/V) methanol, and 230 ng/L surrogates). If necessary, samples were diluted with Milli-Q water when transferred to autosampler vials. For the LC–MS/MS analysis, 1 mL samples were directly injected onto a Gemini 50 × 4.6 mm C18 column 1 with 3 μm particle size and 100 Å pore size (Phenomenex). All PFASs were measured by electrospray ionization (ESI) operated in negative mode. The five PFCAs and four PFASs quantified by LC–MS/MS and their corresponding surrogates are listed in Table S3; all other PFASs were measured using LC–QToF-MS (described below). Eluents for the gradient method were 10 mM ammonium acetate in water and 10 mM ammonium acetate in methanol, prepared using all LC–MS grade materials. Additional details on the instruments and methods used for LC–MS/MS and LC–QToF-MS analysis are shown in Tables S4 and S5. The calibration curve ranged from 0.77 to ~7700 ng/L, and peak area data was analyzed by MultiQuant 3.1 software with a 1/*x*² weighting and an accuracy tolerance of 30% for calibration curves. Double blanks (without surrogate nor standards), blanks (with surrogate but not standards), and quality control (QC) samples (with surrogates and standards) were included in the analytical sequence every 8–10 samples to ensure minimal contamination and adequate MS performance. Only signals (i.e., peak areas) greater than 10 times any background signals observed in the blanks or double blanks were considered acceptable and used for subsequent data analysis.

Samples for LC–QToF-MS analysis were similarly prepared and directly injected (1 mL) onto a Gemini 100 × 3 mm C18 column with 3 μm particle size and 100 Å pore size, (Phenomenex) and measured by ESI operated in negative mode with a collision energy of –60 V. The compounds listed in Table 1 as analyzed by LC–QToF-MS were identified using a custom-built library in Masterview 1.1 software with a peak

intensity threshold of 1000 cps and a minimum signal-to-noise ratio of 10. After the extraction of candidate peaks using broad criteria (XIC width of 0.02 Da and retention time width of 0.9 min), compound identification was performed by comparison to the MS spectral library, with Masterview-generated MS spectral library scores required to be greater than 85/100 and a 5 ppm mass error tolerance of precursor ion formulae. This library was the result of previously described PFAS discovery work.^{25,29} For PFASs identified using this library for which no authentic standards were available at the time of analysis (20 of the 21 PFASs measured via LC-QToF-MS), a (relative) semiquantitative approach was applied: the calibration curve was generated by diluting different volumes of the original groundwater to a final volume of 1.3 mL (containing 20 vol % methanol and 3 mg/L NH₄OH). For the samples themselves, 0.7 mL was added to a final volume of 1.3 mL (containing 20 vol % methanol and 3 mg/L NH₄OH) and compared to this dilution–calibration curve for relative quantification. Additionally, 6:2 fluorotelomer sulfonate (6:2 FtS), for which a standard was available, was also quantified by LC-QToF-MS (using the accurate mass of the parent ion), but standard calibration curves were used for quantification in a manner identical to that described for the LC-MS/MS analysis.

Batch Experiments for Sorbent Screening and Kinetics. Similar to the sorbent screening approach employed by Ulrich et al.,⁴² 5 day batch sorption experiments were carried out to screen the eight carbonaceous sorbents for PFAS sorptive affinity using unfiltered AFFF-impacted groundwater. Though equilibrium was not expected in 5 days; the intent was merely to compare the relative sorptive affinity of the different sorbents. As described in the [Supporting Information](#), preliminary studies were conducted to identify an appropriate solid to water ratio to obtain an adequate removal percentage of targeted compounds (>10%) without falling below the limits of quantification (LOQs), which were analyte-dependent but typically 0.77 to 38.5 ng/L ([Table S3](#)). For subsequent studies, batch experiments were prepared by first adding 5 mg of each sorbent to 50 mL polypropylene centrifuge tubes. Preliminary results ([Figure S1](#)) suggested that a solid-to-liquid ratio of 5 mg to 50 mL was sufficient to remove weakly sorbing PFASs (i.e., PFBS) while still allowing sufficient quantities of the strongly sorbing PFASs (i.e., PFOS). After purging with CO₂ to minimize bubbles,⁴⁴ 50 mL of groundwater with 0.5 mL of 20 g/L sodium azide (final NaN₃ concentration in mixture: 200 mg/L) was added to inactivate microbial activity (concentration chosen to minimize effects on sorption according to previous studies).^{42,45,46} All experimental conditions (time points, carbon doses, etc.) were prepared in triplicate. After 5 days of vigorous shaking on 1 at ambient temperature (~22 °C), subsamples were taken for LC-MS/MS and LC-QToF-MS analysis.

For the sorbent F300, the sorbent-groundwater mixture (with NaN₃) was shaken and subsampled (after settling for 15 min) at various time points for kinetic tests (2 h and 0.5, 1, 2, 3, 5, 10, 20, and 30 days). To compare the effectiveness of F300 for sorption of the different PFASs under closer-to-equilibrium conditions, a 20 day partition coefficient (20d- K_d) was calculated by dividing the sorbed concentration (q_t , determined by the aqueous loss method, [Equation S2](#)) by the aqueous concentration (c_t) for each PFAS. For PFASs for which quantitation was not possible (due to lack of authentic standards), the relative peak area, as opposed to the relative

concentration, was instead used to calculate the K_d values ([Table S6](#)).

Model Calibration. The intraparticle diffusion kinetic model was applied to describe the sorption kinetics observed for F300. The kinetic model input included the molecular weight (MW) of each compound as well as the effective particle radius (0.045 cm), intraparticle porosity (0.59), and solid density (2.0 g/cm³) for F300 (measured or estimated previously).⁴² The kinetic model was then calibrated to the kinetic data (day 30 data, which was not available for several compounds, was not included to avoid potential biases among PFASs) for all PFASs that exhibited consistent kinetic profiles that could be fit by the intraparticle diffusion model, according to the method described by Ulrich et al. (calibrated for all compounds except PFBA, 6:2 FtS, N-SPAmP-FBSA, and N-SHOPAmP-FBSA; details in the [Supporting Information](#)).^{42,47} This was carried out by (1) estimating equilibrium K_d values (described below) and then (2) using Matlab to fit the nonlinear intraparticle diffusion kinetic model (with the equilibrium K_d as an input) by adjusting the “apparent tortuosity” to minimize the sum of squared residuals (SSR). While the actual tortuosity is a physical property of the sorbent (describing its pore-interconnectivity), this apparent tortuosity was used to account for observed differences among PFASs (discussed later). For PFASs that did not appear to approach equilibrium in the kinetic experiments, an equilibrium K_d was estimated with the linearized pseudo second-order kinetic model (normalized to fit peak area data; [eq S4](#))^{47–49} to avoid ambiguity from fitting multiple parameters simultaneously. It is important to note that this linearized model is known to underestimate equilibrium K_d , particularly for systems that are far from equilibrium;⁵⁰ thus, results should be interpreted with this potential bias in mind.

Full-Scale System Simulations. Forward predictions were carried out to simulate a GAC adsorption system treating AFFF-impacted water identical in size and operation to a system that was monitored for PFAS breakthrough in a previous study³⁰ to confirm that the predicted bed volumes to breakthrough (BV_{BT}) were on the same order of magnitude as previously observed values. The simulated system consisted of a pair of 28.5 m³ vessels operating in series at 1.5 m³/min, each containing 2.7 m of GAC (the model was calibrated for F300, but Calgon F600 was used in the actual system) with an empty-bed contact time (EBCT) of 13 min (26 min EBCT overall). The calibrated transport model describing sorption-retarded, intraparticle diffusion-limited transport of the PFASs in a GAC bed was applied as described by Ulrich et al. 2015 (adapted from a model originally described by Werner et al. 2012; see the [Supporting Information](#) for additional details).^{42,51} To assess the importance of intraparticle diffusion limitations, breakthrough predictions were compared to those from the transport model when it was simplified to assume localized sorption equilibrium. Furthermore, a dimensionless number representing the ratio between advective travel time and diffusion time was calculated for each PFAS (i.e., diffusion limitations are expected if the “Peclet number” calculated by [eq S8](#) is greater than 1).^{51,52}

RESULTS AND DISCUSSION

Sorbent Screening. For initial screening experiments to assess the relative removal performance among all evaluated sorbents and particle sizes, aqueous PFAS concentrations after 5 days of equilibration were measured and compared. Example

results for PFOA and PFOS are reported in Figure 1, as these PFASs were present at the highest concentrations among their

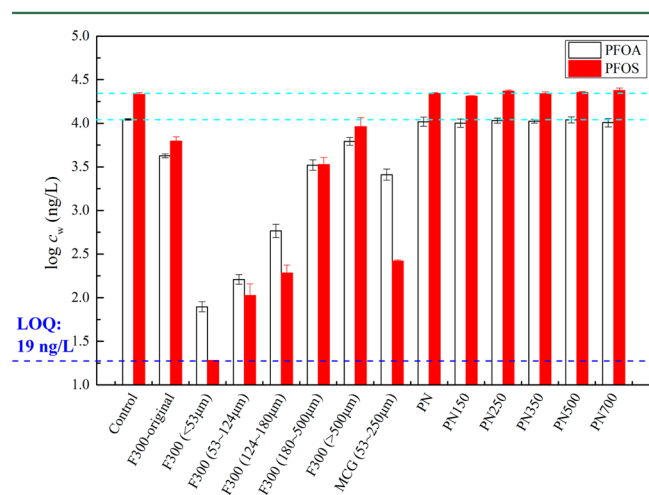


Figure 1. Logarithmic aqueous PFOA and PFOS concentrations ($\log c_w$) after 5 days of equilibration with F300 GAC (at varying particle size fractions), MCG-biochar, and PN-biochar (produced at various temperatures).

respective structural classes in this AFFF-impacted water supply ($\sim 11\,000$ and $\sim 33\,000$ ng/L, respectively; Table S2). As depicted in Figure 1, the sorptive removal of PFOA and PFOS after 5 days of equilibration was quite variable among the sorbents. Despite the higher initial concentration of PFOS as compared to PFOA, lower PFOS concentrations were observed after 5 days of equilibration for most cases in which adsorptive removal was observed. This indicates a higher sorptive affinity for PFOS, as has been observed previously for carbonaceous sorbents.^{9,30,40} A particle size effect was also evident for F300: finer particle sizes demonstrated greater removal of PFOS and PFOA after 5 days of equilibration. This potentially indicates intraparticle sorption limitations, particularly for larger particle sizes.⁵³ Overall, these results indicated that F300 and MCG-biochar were much more effective for removal of PFOA and PFOS from groundwater than PN-derived biochars. This was likely due to the materials' higher SA (Table S1) as well as the superior ability of their more aromatic surfaces to sorb the PFASs via hydrophobic interactions.^{42,54} The good performance of MCG-biochar is notable, as it indicates that high-SA biochars could potentially serve as alternatives to GAC. However, as biochar properties are more widely variable than those of commercially available GACs, subsequent kinetic modeling efforts focused on F300.

20 Day K_d Values for Sorption to F300. Figure 2 shows a comparison of the 20 day $\log K_d$ values for sorption of the analyzed PFASs onto F300. PFHpS and PFOS showed the highest K_d values among the analyzed PFASs, with all of the newly discovered PFASs demonstrating lower K_d values. As has been observed previously for the PFCAs and PFSAs,^{3,40} an increase in perfluoroalkyl chain length generally resulted in increases in the 20 day $\log K_d$ values for PFAS classes with simple head groups (i.e., PFCAs, PFSAs, FTSs, and FASAs; Figures 2 and S2). However, this trend is less clear for PFAS classes with more-complex head groups. For example, longer-chained homologues among the *N*-sulfoethyl dimethylammonioethyl perfluoroalkanesulfonamides (*N*-SPAmP-FASAs) and the *N*-sulfohydroxypropyl dimethylammonioethyl per-

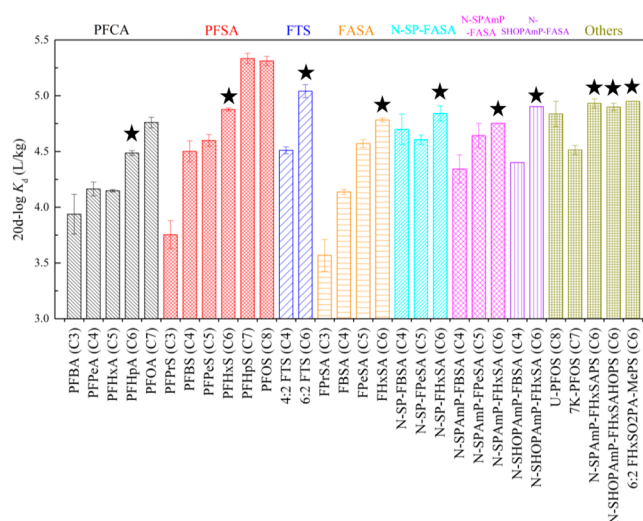


Figure 2. 20 day $\log K_d$ for sorption of the analyzed PFASs onto F300-original. The stars denote PFASs with a six-carbon perfluoroalkyl moiety (i.e., $F-(CF_2)_6-R$). See Table S7 for tabulated data. Note: The 10 day $\log K_d$ is displayed for 6:2 FHxSO₂PA-MePS because its peak area was not discernible from background after 20 days of equilibration.

fluoroalkanesulfonamides (*N*-SHOPAmP-FASAs) are more strongly sorbed than their shorter-chained counterparts, whereas an increase in perfluoroalkyl chain length for the homologues among the *N*-sulfoethyl perfluoroalkanesulfonamides (*N*-SP-FASAs) did not lead to increased sorption (Figures 2 and S2). Somewhat surprisingly, if PFASs with a perfluorohexyl moiety are compared, 6:2 FtS demonstrated the highest 20 day $\log K_d$ value, despite the fact that many of the other C6-based PFASs have much larger head groups. The calculated K_d values for these polyfluorinated compounds suggests that for a given perfluoroalkyl tail length, there is not a high degree of variability among the PFASs examined here with respect to their sorptive affinity for F300, at least over 20 days. This is likely a result of the competing effects of higher MW head groups that also contain polar or charged functional groups.

A pair of PFOS-like PFASs were also observed in the AFFF-impacted groundwater and were removed, to some extent, by F300. Both unsaturated PFOS (U-PFOS) and a ketone derivative (7K-PFOS; structures shown in Table 1) have been detected in AFFF or AFFF-impacted groundwater, presumably as impurities in the AFFF production process.²⁵ Both PFOS-like compounds exhibit lower 20 day $\log K_d$ values as compared to PFOS (Figure 2), indicating a weaker sorption onto the F300. This is particularly important, as the bioaccumulation potential and toxicity of these PFOS-like compounds is unknown; their mere presence in AFFF-impacted groundwater suggests they exhibit some persistence once released to the environment.

Kinetics for Sorption to F300. Aqueous concentrations of PFASs generally decreased over 30 days of contact with F300 (representative results in Figure 3; complete results in Figures S3 and S4). Figure 3a compares the kinetics of perfluorobutyl-based (i.e., $F-(CF_2)_4-R$) and perfluorohexyl-based PFCAs, PFSAs, and FASAs. PFPeA and *N*-SHOPAmP-FBSA were the most obvious exceptions to the trend of decreasing concentrations over time, with significant concentration increases being observed after 20 and 5 days, respectively

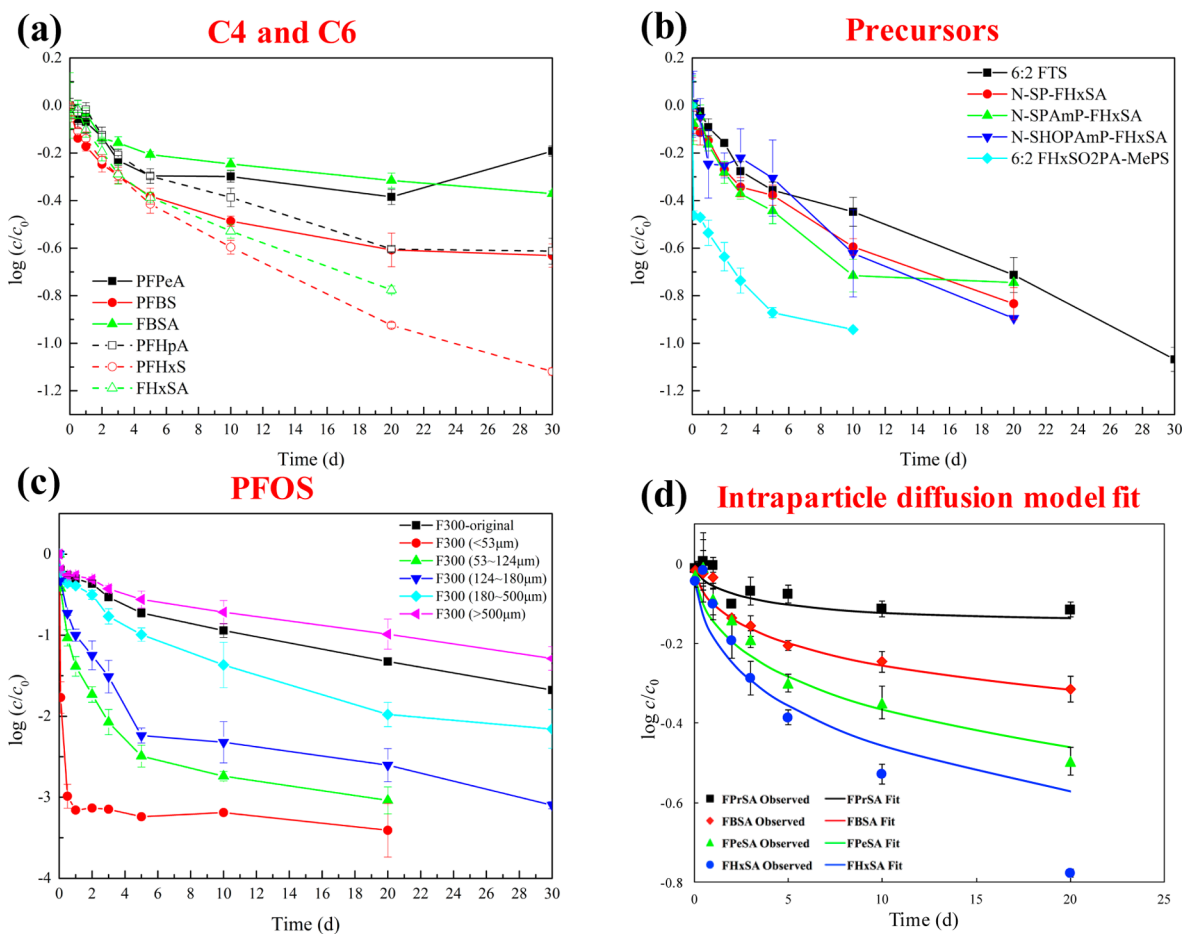


Figure 3. Kinetics of sorption of (a) perfluorobutyl-based and perfluorohexyl-based PFCAs, PFSAs, and FASAs, (b) perfluorohexyl-based precursors, and (c) PFOS on F300-original. Panel c also displays the effect of different sizes of F300 particles on PFOS sorption kinetics. Panel d shows example fits of the intraparticle diffusion model to the kinetic data for the sulfonamides.

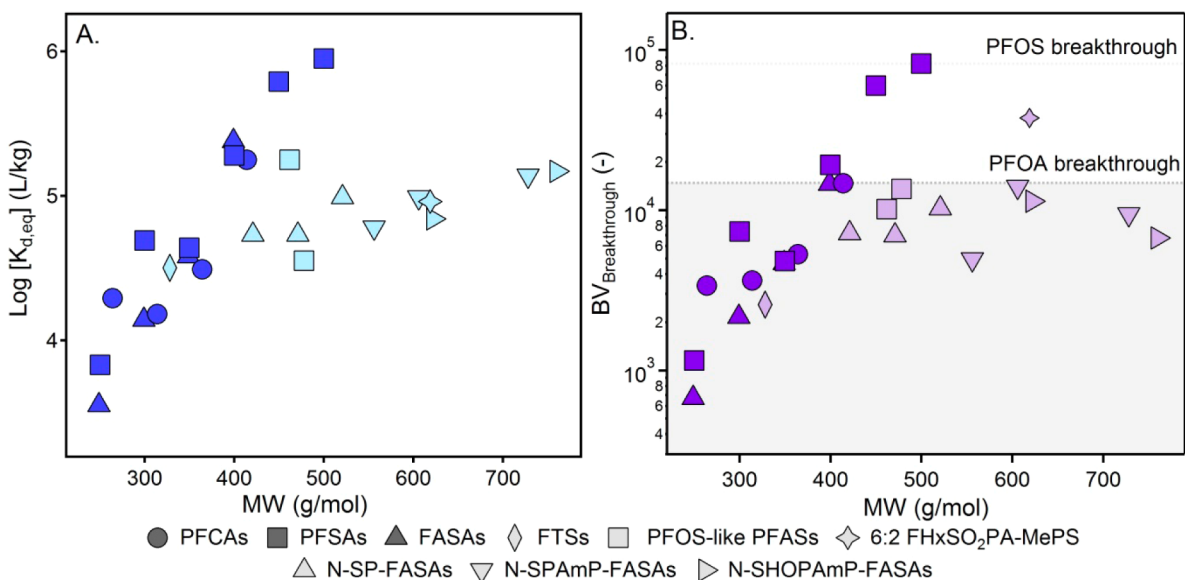


Figure 4. (A) Batch kinetic model calibration results for equilibrium $\log K_{d,eq}$ ($\log [K_{d,eq}]$, Table S6) and (B) results for case-study simulations with the diffusion-limited transport model (reported as predicted bed volumes to breakthrough, $BV_{Breakthrough}$, defined as when $C/C_0 > 0.05$). Shaded areas in panel B indicate compounds predicted to breakthrough before PFOS (lighter shading) and PFOA (darker shading). Perfluorinated compounds are indicated with darker markers, and polyfluorinated compounds and PFOS-like PFASs are indicated with lighter markers.

(Figure S4). It is unclear whether this behavior was caused by competition-induced desorption, formation from a precursor

due to reaction with NaN_3 , or a combination of both processes. Importantly, the kinetic profiles observed for many of the

perfluorohexyl-based precursors were very similar (Figure 3B), with the notably faster kinetics observed for 6:2 FHxSO₂PA–MePS. Though it is one of the larger PFASs (Table 1), 6:2 FHxSO₂PA–MePS is similar in size (and general structure) to N-SHOPAmP–FHxSA, which followed the kinetic profile of the other perfluorohexyl-based PFASs. However, the 3 dayK_d value ($6.5 \pm 0.5 \times 10^4$ L/kg) of 6:2 FHxSO₂PA–MePS is much higher than even that of PFOS ($2.4 \pm 0.2 \times 10^4$ L/kg). It is possible that the highly polarizable amide group unique to 6:2 FHxSO₂PA–MePS brought about its superior sorptive affinity.⁵ Faster sorption rates were observed with smaller particle sizes (Figure 3C shows example behavior for PFOS), potentially indicating intraparticle diffusion limitations, as compounds must diffuse further into larger particles to access intraparticle sorption sites.

Kinetic Model Calibration. The intraparticle diffusion kinetic model was in good agreement with the kinetic data, as the root-mean-square error (RMSE) between observed and predicted C/C₀ was less than 0.03 for all compounds (Table S6). Examples of model fits for the FASAs are shown in Figure 3D. Better fits (lower RMSE values) were obtained for the shorter chain compounds (e.g., better fits to FPrSA and FBSA than FPeSA and FHxSA in Figure 3D). This may have been due to more-pronounced nonlinear sorption effects for larger compounds, causing the outermost GAC sorption sites to become more relevant as the outer aqueous PFAS concentrations decreased over time.⁵⁵ As expected, the calibrated equilibrium K_d values generally increased with MW (Figure 4A). Interestingly, the polyfluorinated compounds did not show as strong of a dependence on MW as did the PFCAs, PFSAs, and FASAs, potentially because their bulkier head groups contained polar moieties or caused increased steric effects.⁵⁶ Apparent tortuosity for most PFASs ranged between 1 and 14 and was generally more variable for larger compounds (Table S6). This could potentially be due to several phenomena, including experimental error, molecular sieving effects (i.e., differences in pore accessibility), or nonlinear sorption causing PFAS uptake rates to change over time. 7K-PFOS and 6:2 FHxSO₂PA–MePS showed exceptionally fast kinetics, with apparent tortuosity values less than 0.5. As tortuosity values less than 1 conflict with classical diffusion theory, these compounds may have not fully diffused into the innermost sorption sites, potentially due to the existence of a branched network of micropores and macropores. Furthermore, as these compounds contain polarizable amide (6:2 FHxSO₂PA–MePS) or ketone (7K-PFOS) groups that enhance their sorptive affinity for carbonaceous surfaces, they may have outcompeted other PFASs or DOC molecules for the outermost sorption sites.

Full-Scale System Simulations. The results of the intraparticle diffusion-limited transport model simulations for the predicted BV_{BT} for each PFAS in a GAC adsorption system are shown in Figure 4B (BV_{BT} predicted by localized equilibrium model is shown in Table S6, and breakthrough curves are shown in Figures S5 and S6). Considering that a previous study observed PFOS breakthrough in an actual full-scale GAC filtration system at approximately 60 000 BVs (from which the dimensions and conditions were selected for the simulations in this study),³⁰ the BV_{BT} values predicted by the intraparticle diffusion-limited transport model (PFOS BV_{BT} of approximately 80 000), were considerably closer to observed values than those predicted by the localized equilibrium transport model (PFOS BV_{BT} of approximately 400 000).

While the model predicted earlier BV_{BT} values than observed in the same study for less strongly sorbed PFASs (i.e., approximately 15 000 BV_{BT} and 3600 BV_{BT} predicted for PFOA and PFHxA, respectively, versus approximately 30 000 BV_{BT} in the full-scale system), the predictions being within an order of magnitude of the field-measured values is notable, as the actual system contained a different GAC and was treating different water (with different levels of PFASs, different DOC, etc.). In particular, higher DOC levels may result in slower sorption kinetics and lower equilibrium K_d values,⁴² making a comparison of results obtained from different waters difficult. Nevertheless, the similarity between the actual breakthrough in a full-scale system and the breakthrough simulated with intraparticle diffusion-limited transport model suggests the model may accurately capture kinetic and sorptive behavior of PFASs in GAC systems.

Despite the apparently strong kinetic sorption effects under the simulated operating conditions, both the intraparticle diffusion-limited model and the local equilibrium model predicted very similar PFAS breakthrough orders. 7K-PFOS and 6:2 FHxSO₂PA–MePS were exceptions, as the diffusion-limited model predicted these compounds to be later in the breakthrough order than the equilibrium model. This is likely because diffusion limitations were less significant for these PFASs for the simulated operating conditions, as they were the only compounds with Peclet numbers above 1 (3.5 and 7.6 for 7K-PFOS and 6:2 FHxSO₂PA–MePS, respectively; Table S6). As both models predicted similar breakthrough orders despite strong kinetic limitations, the relative affinity of the various PFASs for GAC may adequately indicate breakthrough order when kinetic tests or column tests are not possible.

It is important to note that competition for sorption sites (between PFASs, as well as PFASs and DOC) may affect breakthrough behavior differently in actual systems than is predicted by the model. For example, a previous study using the same model found that batch calibration experiments at higher DOC levels provided better predictions for observed breakthrough behavior in column verification experiments,¹ suggesting that continuous loading with DOC may lead to greater fouling effects that are not described in the model. Furthermore, smaller compounds may initially appear to be more strongly retained because they reach portions of virgin carbon before DOC or larger PFASs, making them susceptible to remobilization over time. Therefore, while the forward-modeling approach used here provides useful qualitative insight, pilot-scale column verification experiments should be conducted if sufficient water quantities are available.

Predicting Removal for Newly Discovered PFASs. While the results discussed above indicate that some polyfluorinated compounds and PFOS-like PFASs may be removed less effectively than PFOS and PFOA during GAC adsorption, efforts to characterize their removal are (currently) limited. This is largely due to the absence of commercial standards, although the detection and identification of these compounds requires sophisticated instrumentation that is not (yet) widely available. For these reasons, it would be useful to relate predicted PFAS removal to more readily observable properties, particularly as it appears that MW is not a good indicator of breakthrough behavior. Thus, in an effort to enable simplified predictions for removal of all PFASs present, we examined the ability of retention time on our analytical C18 column (RT_{C18}) to predict a compound's breakthrough behavior (similar to using relative chromatographic retention

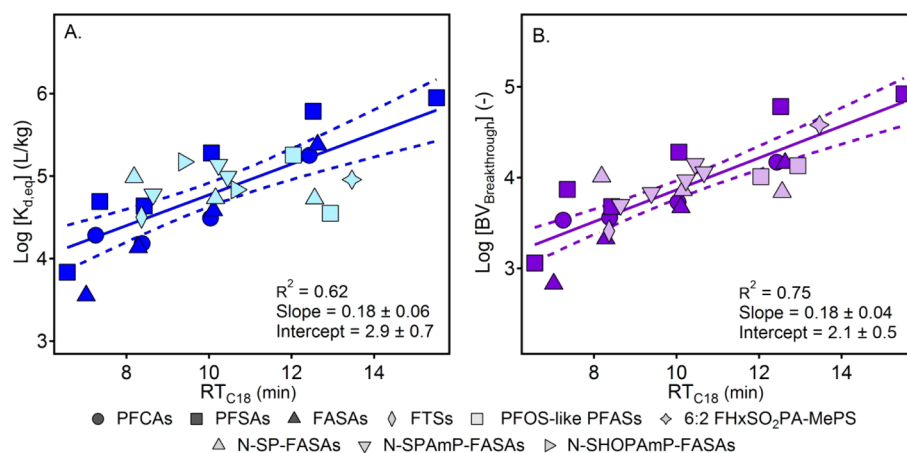


Figure 5. (A) Equilibrium $\log K_d$ ($\log [K_{d,eq}]$) versus retention time on a C18 column (RT_{C18}). (B) Logarithm of the predicted bed volumes to breakthrough ($BV_{Breakthrough}$, defined as when $C/C_0 > 0.05$) from the diffusion-limited transport model versus RT_{C18} . Perfluorinated compounds are indicated with darker markers, and polyfluorinated compounds and PFOS-like PFASs are indicated with lighter markers. Linear regressions are indicated with solid lines, and the 95% confidence interval is indicated with dotted lines. Retention times are provided in Table S7.

to predict a partition coefficient⁵⁷), as we expect RT_{C18} to mimic, to some extent, the van der Waals interactions between the solute and sorbent (C18 versus F300) as well as kinetic effects experienced during transport.

To this end, linear regressions were evaluated for RT_{C18} versus the calibrated equilibrium K_d values (Figure 5A) as well as BV_{BT} values predicted by the diffusion-limited transport model (Figure 5B). RT_{C18} appeared to be a much-better indicator of equilibrium K_d and BV_{BT} than MW, potentially because the steric effects of the bulky head groups on the polyfluorinated compounds could be better taken into account. Moreover, the linear relationship with RT_{C18} appeared to be better for BV_{BT} than for equilibrium K_d , suggesting that RT_{C18} may also account for kinetic transport effects, at least to some degree. Importantly, however, improved regressions for equilibrium K_d and BV_{BT} versus MW (rather than RT_{C18}) may be obtained among the PFCAs, PFSAs, and FASAs (i.e., Figures 4, S7, and S8). Overall, these results suggest that linear relationships with RT_{C18} may provide an acceptable and relatively simple method to predict relative GAC sorption affinity and breakthrough behavior for the broader suite of AFFF-derived PFASs.

ENVIRONMENTAL IMPLICATIONS

Trends in model predictions among the different PFASs bring to light some interesting, although not entirely unexpected, implications. An especially important observation is that many shorter-chain but also polyfluorinated compounds were predicted to break through GAC sorption systems before PFOA and PFOS by thousands of bed volumes for some compounds. While the earlier breakthrough of shorter-chain PFCAs and PFSAs has been well-documented,³⁰ very little data are available for polyfluorinated compounds and PFOS-like compounds. This is generally more of a concern for the polyfluorinated compounds and the PFOS-like PFASs (U-PFOS and 7K-PFOS) than the shorter-chain PFCAs and PFSAs, as the shorter-chain PFCAs and PFSAs tend to be less bioaccumulative, though toxicity data are still very much lacking for all of these chemicals.⁵⁸ These findings may only scratch the surface of the potential risks associated with these newly discovered polyfluorinated precursors and PFOS-like PFASs: it is quite possible that some of these chemicals are widely

present in AFFF-impacted groundwater intended for human consumption, yet their toxicity, actual concentration, and potential for bioaccumulation remains largely unknown. Fortunately, the data presented here suggest that there may be appropriate control measures to reduce the potential exposure of populations consuming AFFF-impacted drinking water. GAC is a commonly employed and, when employed correctly, effective treatment technology for communities impacted by PFAS-contaminated drinking water, although alternative drinking water treatment technologies such as membranes may be more effective for the broader suite of PFASs.³⁰ In the cases in which GAC treatment is advantageous from a cost or operational perspective, the shorter-chain and easily measurable PFASs such as PFBA, rather than PFOS or PFOA, could be monitored to inform the potential for breakthrough of these shorter-chain PFASs as well as polyfluorinated and PFOS-like PFASs. Though not without significant additional cost, the change-out of GAC based on shorter-chain PFASs could ensure greater protection from potential exposure to PFASs as a whole, including the newly discovered polyfluorinated precursors and PFOS-like PFASs of unknown concentration, bioaccumulation potential, and toxicity.

ASSOCIATED CONTENT

Supporting Information

The Supporting Information is available free of charge on the ACS Publications website at DOI: 10.1021/acs.est.7b00970.

Additional details of materials and methods. Tables showing surface and production characteristics, concentrations in AFFF-impacted groundwater, standard and surrogate purity and typical limits of quantification, an HPLC gradient, operating conditions, fitting results, and retention times. Figures showing c/c_0 variations, relationships between chain length and K_d , kinetics data, breakthrough curves, and retention times vs F300 $\log K_d$. (PDF)

AUTHOR INFORMATION

Corresponding Author

*Phone: (720)-984-2116; fax: (303)-273-3413; e-mail: chiggins@mines.edu.

ORCID 

Baoliang Chen: 0000-0001-8196-081X

Christopher P. Higgins: 0000-0001-6220-8673

Notes

The authors declare no competing financial interest.

ACKNOWLEDGMENTS

We thank the scholarship support for X.X. from the China Scholarship Council. We thank Dr. Aniela Burant from the Colorado School of Mines (CSM) for help in sample analysis and Dr. Krista Barzen-Hanson of Oregon State University (OSU) for help in identifying the PFASs. This project was supported by the National Natural Science Foundations of China (grant no. 21425730). We also thank D. Werner of Newcastle University; C. Schaefer of CDM Smith; T. Cath and C. Bellona of CSM; J. Field and K. Barzen-Hanson of OSU; and S. Gormley, S. Thomas, and B. Malyk of AMEC Foster-Wheeler for helpful comments during the development of this manuscript.

REFERENCES

- Moody, C. A.; Field, J. A. Perfluorinated surfactants and the environmental implications of their use in fire-fighting foams. *Environ. Sci. Technol.* **2000**, *34* (18), 3864–3870.
- Karrman, A.; Elgh-Dalgren, K.; Lafossas, C.; Moskeland, T. Environmental levels and distribution of structural isomers of perfluoroalkyl acids after aqueous fire-fighting foam (AFFF) contamination. *Environ. Chem.* **2013**, *8* (4), 372–380.
- Guelfo, J. L.; Higgins, C. P. Subsurface transport potential of perfluoroalkyl acids at aqueous film-forming foam (AFFF)-impacted sites. *Environ. Sci. Technol.* **2013**, *47* (9), 4164–4171.
- Hu, X. C.; Andrews, D. Q.; Lindstrom, A. B.; Bruton, T. A.; Schaidler, L. A.; Grandjean, P.; Lohmann, R.; Carignan, C. C.; Blum, A.; Balan, S. A.; et al. Detection of poly- and perfluoroalkyl substances (PFASs) in US drinking water linked to industrial sites, military fire training areas, and wastewater treatment plants. *Environ. Sci. Technol. Lett.* **2016**, *3* (10), 344–350.
- Houtz, E. F.; Sutton, R.; Park, J. S.; Sedlak, M. Poly- and perfluoroalkyl substances in wastewater: Significance of unknown precursors, manufacturing shifts, and likely AFFF impacts. *Water Res.* **2016**, *95*, 142–149.
- Houtz, E. F.; Higgins, C. P.; Field, J. A.; Sedlak, D. L. Persistence of perfluoroalkyl acid precursors in AFFF-impacted groundwater and soil. *Environ. Sci. Technol.* **2013**, *47* (15), 8187–8195.
- Place, B. J.; Field, J. A. Identification of novel fluorochemicals in aqueous film-forming foams used by the US military. *Environ. Sci. Technol.* **2012**, *46* (13), 7120–7127.
- Giesy, J. P.; Kannan, K. Perfluorochemical surfactants in the environment. *Environ. Sci. Technol.* **2002**, *36* (7), 146a–152a.
- Zareitalabad, P.; Siemens, J.; Hamer, M.; Amelung, W. Perfluorooctanoic acid (PFOA) and perfluorooctanesulfonic acid (PFOS) in surface waters, sediments, soils and wastewater - A review on concentrations and distribution coefficients. *Chemosphere* **2013**, *91* (6), 725–732.
- Post, G. B.; Cohn, P. D.; Cooper, K. R. Perfluorooctanoic acid (PFOA), an emerging drinking water contaminant: A critical review of recent literature. *Environ. Res.* **2012**, *116*, 93–117.
- Yao, Y. M.; Sun, H. W.; Gan, Z. W.; Hu, H. W.; Zhao, Y. Y.; Chang, S.; Zhou, Q. X. Nationwide distribution of per- and polyfluoroalkyl substances in outdoor dust in mainland China from eastern to western areas. *Environ. Sci. Technol.* **2016**, *50* (7), 3676–3685.
- U.S. EPA. *Lifetime health advisories and health effects support documents for perfluorooctanoic acid and perfluorooctane sulfonate*; Environmental Protection Agency: Washington, DC, 2016.
- U.S. EPA. FACT SHEET PFOA & PFOS Drinking water health advisories. https://www.epa.gov/sites/production/files/2016-06/documents/drinkingwaterhealthadvisories_pfoa_pfos_updated_5.31.16.pdf (accessed May 7, 2017).
- U.S. EPA. Unregulated contaminant monitoring rule 3 (UCMR 3). <https://www.epa.gov/dwucmr/third-unregulated-contaminant-monitoring-rule> (accessed May 7, 2017).
- Hurley, S.; Houtz, E.; Goldberg, D.; Wang, M. M.; Park, J. S.; Nelson, D. O.; Reynolds, P.; Bernstein, L.; Anton-Culver, H.; Horn-Ross, P.; Petreas, M. Preliminary associations between the detection of perfluoroalkyl acids (PFAAs) in drinking water and serum concentrations in a sample of California women. *Environ. Sci. Technol. Lett.* **2016**, *3* (7), 264–269.
- Grandjean, P.; Heilmann, C.; Weihe, P.; Nielsen, F.; Mogensen, U. B.; Budtz-Jørgensen, E. Serum vaccine antibody concentrations in adolescents exposed to perfluorinated compounds. *Environ. Health Perspect* **2016**, *10.1289/EHP275*
- Timmermann, C. A. G.; Budtz-Jørgensen, E.; Petersen, M. S.; Weihe, P.; Steuerwald, U.; Nielsen, F.; Jensen, T. K.; Grandjean, P. Shorter duration of breastfeeding at elevated exposures to perfluoroalkyl substances. *Reprod. Toxicol.* **2017**, *68*, 164–170.
- Agency of Natural Resources. Chapter 12 of the Environmental Protection Rules: Groundwater Protection Rule and Strategy. http://dec.vermont.gov/sites/dec/files/documents/2016_12_16_GWPR%26Sadoption.pdf (accessed May 7, 2017).
- Rhoads, K. R.; Janssen, E. M. L.; Luthy, R. G.; Criddle, C. S. Aerobic biotransformation and fate of N-ethyl perfluorooctane sulfonamidoethanol (N-EtFOSE) in activated sludge. *Environ. Sci. Technol.* **2008**, *42* (8), 2873–2878.
- D'eon, J. C.; Mabury, S. A. Production of perfluorinated carboxylic acids (PFCAs) from the biotransformation of polyfluoroalkyl phosphate surfactants (PAPS): Exploring routes of human contamination. *Environ. Sci. Technol.* **2007**, *41* (13), 4799–4805.
- Avendano, S. M.; Liu, J. X. Production of PFOS from aerobic soil biotransformation of two perfluoroalkyl sulfonamide derivatives. *Chemosphere* **2015**, *119*, 1084–1090.
- D'eon, J. C.; Mabury, S. A. Exploring indirect sources of human exposure to perfluoroalkyl carboxylates (PFCAs): Evaluating uptake, elimination, and biotransformation of polyfluoroalkyl phosphate esters (PAPs) in the rat. *Environ. Health Persp.* **2010**, *119* (3), 344–350.
- Fakouri Baygi, S.; Crimmins, B. S.; Hopke, P. K.; Holsen, T. M. Comprehensive emerging chemical discovery: Novel polyfluorinated compounds in lake Michigan trout. *Environ. Sci. Technol.* **2016**, *50* (17), 9460–9468.
- D'Agostino, L. A.; Mabury, S. A. Identification of novel fluorinated surfactants in aqueous film forming foams and commercial surfactant concentrates. *Environ. Sci. Technol.* **2014**, *48* (1), 121–129.
- Barzen-Hanson, K. A.; Roberts, S. C.; Choyke, S.; Oetjen, K.; McAlees, A.; Riddell, N.; McCrindle, R.; Ferguson, P. L.; Higgins, C. P.; Field, J. A. Discovery of 40 classes of per- and poly-fluoroalkyl substances in historical aqueous film-forming foams (AFFF) and AFFF-impacted groundwater. *Environ. Sci. Technol.* **2017**, *51* (4), 2047–2057.
- McGuire, M. E.; Schaefer, C.; Richards, T.; Backe, W. J.; Field, J. A.; Houtz, E.; Sedlak, D. L.; Guelfo, J. L.; Wunsch, A.; Higgins, C. P. Evidence of remediation-induced alteration of subsurface poly- and perfluoroalkyl substance distribution at a former firefighter training area. *Environ. Sci. Technol.* **2014**, *48* (12), 6644–6652.
- Schultz, M. M.; Barofsky, D. F.; Field, J. A. Quantitative determination of fluorotelomer sulfonates in groundwater by LC MS/MS. *Environ. Sci. Technol.* **2004**, *38* (6), 1828–1835.
- Phillips, M. M.; Dinglasan-Panlilio, M. J. A.; Mabury, S. A.; Solomon, K. R.; Sibley, P. K. Fluorotelomer acids are more toxic than perfluorinated acids. *Environ. Sci. Technol.* **2007**, *41* (20), 7159–7163.
- Rotander, A.; Karrman, A.; Toms, L. M. L.; Kay, M.; Mueller, J. F.; Ramos, M. J. G. Novel fluorinated surfactants tentatively identified in firefighters using liquid chromatography quadrupole time-of-flight tandem mass spectrometry and a case-control approach. *Environ. Sci. Technol.* **2015**, *49* (4), 2434–2442.

- (30) Appleman, T. D.; Higgins, C. P.; Quinones, O.; Vanderford, B. J.; Kolstad, C.; Zeigler-Holady, J. C.; Dickenson, E. R. V. Treatment of poly- and perfluoroalkyl substances in US full-scale water treatment systems. *Water Res.* **2014**, *51*, 246–255.
- (31) Appleman, T. D.; Dickenson, E. R. V.; Bellona, C.; Higgins, C. P. Nanofiltration and granular activated carbon treatment of perfluoroalkyl acids. *J. Hazard. Mater.* **2013**, *260*, 740–746.
- (32) Deng, S. B.; Yu, Q. A.; Huang, J.; Yu, G. Removal of perfluorooctane sulfonate from wastewater by anion exchange resins: Effects of resin properties and solution chemistry. *Water Res.* **2010**, *44* (18), 5188–5195.
- (33) Lampert, D. J.; Frisch, M. A.; Speitel, G. E., Jr Removal of perfluorooctanoic acid and perfluorooctane sulfonate from wastewater by ion exchange. *Pract. Period. Hazard. Toxic, Radioact. Waste Manage.* **2007**, *11* (1), 60–68.
- (34) Steinle-Darling, E.; Reinhard, M. Nanofiltration for trace organic contaminant removal: Structure, solution, and membrane fouling effects on the rejection of perfluorochemicals. *Environ. Sci. Technol.* **2008**, *42* (14), 5292–5297.
- (35) Tang, C. Y. Y.; Fu, Q. S.; Robertson, A. P.; Criddle, C. S.; Leckie, J. O. Use of reverse osmosis membranes to remove perfluorooctane sulfonate (PFOS) from semiconductor wastewater. *Environ. Sci. Technol.* **2006**, *40* (23), 7343–7349.
- (36) Stackelberg, P. E.; Gibbs, J.; Furlong, E. T.; Meyer, M. T.; Zaugg, S. D.; Lippincott, R. L. Efficiency of conventional drinking-water-treatment processes in removal of pharmaceuticals and other organic compounds. *Sci. Total Environ.* **2007**, *377* (2–3), 255–272.
- (37) Huerta-Fontela, M.; Galceran, M. T.; Ventura, F. Occurrence and removal of pharmaceuticals and hormones through drinking water treatment. *Water Res.* **2011**, *45* (3), 1432–1442.
- (38) Yu, Q.; Zhang, R. Q.; Deng, S. B.; Huang, J.; Yu, G. Sorption of perfluorooctane sulfonate and perfluorooctanoate on activated carbons and resin: Kinetic and isotherm study. *Water Res.* **2009**, *43* (4), 1150–1158.
- (39) Sun, M.; Arevalo, E.; Strynar, M.; Lindstrom, A.; Richardson, M.; Kearns, B.; Pickett, A.; Smith, C.; Knappe, D. R. U. Legacy and emerging perfluoroalkyl substances are important drinking water contaminants in the Cape Fear river watershed of North Carolina. *Environ. Sci. Technol. Lett.* **2016**, *3* (12), 415–419.
- (40) Higgins, C. P.; Luthy, R. G. Sorption of perfluorinated surfactants on sediments. *Environ. Sci. Technol.* **2006**, *40* (23), 7251–7256.
- (41) Wang, F.; Shih, K. M. Adsorption of perfluorooctanesulfonate (PFOS) and perfluorooctanoate (PFOA) on alumina: Influence of solution pH and cations. *Water Res.* **2011**, *45* (9), 2925–2930.
- (42) Ulrich, B. A.; Im, E.; Werner, D.; Higgins, C. P. Biochar and activated carbon for enhanced trace organic contaminant retention in stormwater infiltration systems. *Environ. Sci. Technol.* **2015**, *49* (10), 6222–6230.
- (43) McKenzie, E. R.; Siegrist, R. L.; McCray, J. E.; Higgins, C. P. Effects of chemical oxidants on perfluoroalkyl acid transport in one-dimensional porous media columns. *Environ. Sci. Technol.* **2015**, *49* (3), 1681–1689.
- (44) Meng, P. P.; Deng, S. B.; Lu, X. Y.; Du, Z. W.; Wang, B.; Huang, J.; Wang, Y. J.; Yu, G.; Xing, B. S. Role of air bubbles overlooked in the adsorption of perfluorooctanesulfonate on hydrophobic carbonaceous adsorbents. *Environ. Sci. Technol.* **2014**, *48* (23), 13785–13792.
- (45) Pignatello, J. J.; Kwon, S.; Lu, Y. F. Effect of natural organic substances on the surface and adsorptive properties of environmental black carbon (char): Attenuation of surface activity by humic and fulvic acids. *Environ. Sci. Technol.* **2006**, *40* (24), 7757–7763.
- (46) Zhu, D. Q.; Kwon, S.; Pignatello, J. J. Adsorption of single-ring organic compounds to wood charcoals prepared under different thermochemical conditions. *Environ. Sci. Technol.* **2005**, *39* (11), 3990–3998.
- (47) Ho, Y. S.; McKay, G. Sorption of dye from aqueous solution by peat. *Chem. Eng. J.* **1998**, *70* (2), 115–124.
- (48) Ho, Y.-S. Review of second-order models for adsorption systems. *J. Hazard. Mater.* **2006**, *136* (3), 681–689.
- (49) Chen, Z.; Chen, B.; Chiou, C. T. Fast and slow rates of naphthalene sorption to biochars produced at different temperatures. *Environ. Sci. Technol.* **2012**, *46* (20), 11104–11111.
- (50) Plazinski, W.; Dziuba, J.; Rudzinski, W. Modeling of sorption kinetics: the pseudo-second order equation and the sorbate intraparticle diffusivity. *Adsorption* **2013**, *19* (5), 1055–1064.
- (51) Werner, D.; Karapanagioti, H. K.; Sabatini, D. A. Assessing the effect of grain-scale sorption rate limitations on the fate of hydrophobic organic groundwater pollutants. *J. Contam. Hydrol.* **2012**, *129*, 70–79.
- (52) Bold, S.; Kraft, S.; Grathwohl, P.; Liedl, R. Sorption/desorption kinetics of contaminants on mobile particles: Modeling and experimental evidence. *Water Resour. Res.* **2003**, *39* (12), 1329–1337.
- (53) Kannan, N.; Sundaram, M. M. Kinetics and mechanism of removal of methylene blue by adsorption on various carbons - a comparative study. *Dyes Pigm.* **2001**, *51* (1), 25–40.
- (54) Kupryianchyk, D.; Hale, S. E.; Breedveld, G. D.; Cornelissen, G. Treatment of sites contaminated with perfluorinated compounds using biochar amendment. *Chemosphere* **2016**, *142*, 35–40.
- (55) Hale, S. E.; Tomaszewski, J. E.; Luthy, R. G.; Werner, D. Sorption of dichlorodiphenyltrichloroethane (DDT) and its metabolites by activated carbon in clean water and sediment slurries. *Water Res.* **2009**, *43* (17), 4336–4346.
- (56) Cornelissen, G.; Haftka, J.; Parsons, J.; Gustafsson, O. Sorption to black carbon of organic compounds with varying polarity and planarity. *Environ. Sci. Technol.* **2005**, *39* (10), 3688–3694.
- (57) Schwarzenbach, R. P.; Gschwend, P. M.; Imboden, D. M. *Environmental Organic Chemistry*, 2nd ed.; John Wiley & Sons, Inc.: New York, 2003.
- (58) Wang, Z. Y.; DeWitt, J. C.; Higgins, C. P.; Cousins, I. T. A never-ending story of per- and polyfluoroalkyl substances (PFASs)? *Environ. Sci. Technol.* **2017**, *51* (5), 2508–2518.